

## 浸渍/共沉淀法对 BaO 改性单 Pd 催化剂净化 甲醇汽油车尾气性能的影响

张雪乔<sup>1,2</sup> 田浩杞<sup>1</sup> 叶芝祥<sup>1</sup> 陈耀强<sup>\*2</sup>

(<sup>1</sup> 成都信息工程学院资源环境学院, 成都 610225)

(<sup>2</sup> 四川大学催化材料科学研究所, 成都 610064)

**摘要:** 采用浸渍和共沉淀两种方法分别制备了 BaO 改性的 Pd/CeO<sub>2</sub>-ZrO<sub>2</sub>-La<sub>2</sub>O<sub>3</sub>-Al<sub>2</sub>O<sub>3</sub> 催化剂。运用 N<sub>2</sub> 吸附-脱附, X 射线衍射 (XRD), H<sub>2</sub> 程序升温还原 (H<sub>2</sub>-TPR), NH<sub>3</sub> 程序升温脱附 (NH<sub>3</sub>-TPD), 透射电子显微镜 (TEM) 和 X 射线光电子能谱 (XPS) 对催化剂进行表征, 并考察其对甲醇, CO, C<sub>3</sub>H<sub>8</sub> 和 NO 的催化性能。活性测试结果表明, BaO 的引入可明显改善 Pd 催化剂对甲醇, CO, C<sub>3</sub>H<sub>8</sub> 和 NO 的催化活性, 且浸渍法最佳, 起燃温度 ( $T_{50}$ ) 分别降低了 43, 31, 45 和 35 °C。XRD, H<sub>2</sub>-TPR 及 XPS 结果表明, 浸渍法引入 BaO 主要通过表面改性方式, 强化 Pd-Ce 界面间的相互作用, 改善催化剂的还原性能, 进而提高催化剂的低温活性; 而共沉淀法则是通过结构改性方式增加 CeO<sub>2</sub> 晶格缺陷, 加速活性氧物种的流动, Ce<sup>3+</sup> 浓度的增加是促使 CO 氧化活性显著提高的主要原因。

**关键词:** 氧化钡; 钯; 铈; 甲醇; 催化转化

中图分类号: O643.36<sup>†</sup>; O643.31

文献标识码: A

文章编号: 1001-4861(2015)01-0166-11

DOI: 10.11862/CJIC.2015.002

## BaO Modified Pd-Based Catalysts: Synthesis by Impregnation/Co-Precipitation and Application in Gasoline-Methanol Exhaust Purification

ZHANG Xue-Qiao<sup>1,2</sup> TIAN Hao-Qi<sup>1</sup> YE Zhi-Xiang<sup>1</sup> CHEN Yao-Qiang<sup>\*2</sup>

(<sup>1</sup> College of Resources and Environment, Chengdu University of Information Technology, Chengdu 610225, China)

(<sup>2</sup> Institute of Catalytic Material Science, Sichuan University, Chengdu 610064, China)

**Abstract:** Barium oxide was developed to modify palladium catalysts supported on CeO<sub>2</sub>-ZrO<sub>2</sub>-La<sub>2</sub>O<sub>3</sub>-Al<sub>2</sub>O<sub>3</sub> (CZLA) compound oxides by impregnation/co-precipitation methods. Low temperature N<sub>2</sub> adsorption-desorption, X-ray diffraction (XRD), H<sub>2</sub>-temperature-programmed reduction (H<sub>2</sub>-TPR), NH<sub>3</sub>-temperature programmed desorption (NH<sub>3</sub>-TPD), transmission electron microscopy (TEM) and X-ray photoelectron spectroscopy (XPS) were employed to characterize the influence of the preparation method on physicochemical properties of the catalyst. Catalytic activity performance for methanol, CO, C<sub>3</sub>H<sub>8</sub> and NO conversion was evaluated. Catalytic activity results show that the addition of BaO has a positive effect on the conversion of all pollutants, and the best results are achieved by the impregnation method. The light-off temperature decreases by 43, 31, 45 and 35 °C, respectively. The XRD, H<sub>2</sub>-TPR and XPS results confirm that the impregnation method is mainly based on the surface modification. The enrichment of Ba<sup>2+</sup> strengthens the Pd-Ce interaction in Pd-Ce interface, promoting the reductive ability, thus increasing the catalytic activity at low temperature. The co-precipitation method results in structure disorder and additional anion vacancies accompanied by the formation of more Ce<sup>3+</sup>, which may be beneficial to the conversion of CO.

**Key words:** barium oxide; palladium; ceria; methanol; catalytic activity removal

收稿日期: 2014-04-24。收修改稿日期: 2014-09-08。

国家自然科学基金 (No.51408076, 11405113), 四川省教育厅重点科研基金 (No.14ZA0163), 成都信息工程学院科研人才基金 (No.J201416) 资助项目。

\*通讯联系人。E-mail: nic7501@scu.edu.cn, Tel: +86 28 85418451; 会员登记号: S06N4556M1006。

Alternative fuels become important research interests owing to an increased concern on environmental protection and the need to reduce the dependency on petroleum oil<sup>[1]</sup>. Methanol (or its mixture with gasoline) has been suggested as an alternative fuel due to its larger octane number and less air pollution<sup>[2]</sup>. Although vehicles operating on the gasoline-methanol fuel produce an exhaust with a lower carbon monoxide (CO), hydrocarbons (HCs) and nitrogen oxides (NO<sub>x</sub>), etc, it emits various partial oxidation products such as formaldehyde and unburned methanol vapor<sup>[3]</sup>, which are harmful to the environment. Therefore, it is crucial to develop an efficient catalyst for purification of methanol, CO, HCs and NO<sub>x</sub>, simultaneously.

Pd-based catalysts have attracted much attention for its lower price, more facilities and higher activity for the oxidation of HCs and CO compared with Rh, Pt-based catalysts. Ceria species widely used in three-way catalysts (TWC) exhibit a multiple effects on catalytic performance, such as increasing in oxygen storage capacity (OSC) of TWC<sup>[4]</sup>, improving CO and NO conversion<sup>[5]</sup>, promoting low temperature water-gas shift<sup>[6]</sup>, stabilizing noble metal dispersion<sup>[7]</sup> and minimizing the thermally induced sintering of supports<sup>[8]</sup>. Hence, increasing attentions are focused on TWC with Pd species as catalytic active sites and ceria as the support<sup>[9-10]</sup>. Barium oxide (BaO) is regarded an effective promoter for improving OSC of ceria-zirconia<sup>[11]</sup>, NO<sub>x</sub> storage capacity<sup>[12]</sup>, and thermal stability of ceria-based catalysts, etc<sup>[13]</sup>. Moreover, BaO can also improve catalytic activity for the conversion of CO, HC, NO<sub>x</sub> in vehicle exhaust<sup>[14]</sup>. So far, there have been available many kinds of introduction methods, including microemulsion<sup>[15]</sup>, sol-gel<sup>[16]</sup>, impregnation<sup>[17]</sup> and co-precipitation methods<sup>[18]</sup>. These preparation methods play an important role in promoting the performance of the catalyst. However, BaO-modified Pd catalysts by different methods to purify methanol exhaust have not yet been reported, to the best of our knowledge.

In the present work, Pd-BaO catalysts modified by impregnation/co-precipitation method were prepared and applied in purification of gasoline-methanol

exhaust. The effect of preparation methods on textural, structural, redox, acidity, electron properties and catalytic performance was investigated.

## 1 Experimental

### 1.1 Catalyst preparation

Ce<sub>0.45</sub>Zr<sub>0.45</sub>La<sub>0.1</sub>O<sub>1.95</sub>-Al<sub>2</sub>O<sub>3</sub> (CZLA) solid solution was prepared by co-precipitation method from the corresponding raw materials: Ce(NO<sub>3</sub>)<sub>3</sub>·6H<sub>2</sub>O, ZrOCO<sub>3</sub>·H<sub>2</sub>O, La(NO<sub>3</sub>)<sub>3</sub>·6H<sub>2</sub>O and Al(NO<sub>3</sub>)<sub>3</sub>·9H<sub>2</sub>O. The precursors with a desired stoichiometric ratio were mixed in an aqueous solution, then ammonia was added dropwise to the obtained mixture until pH=10 under vigorous agitation. The precipitates were filtered, washed, dried at 105 °C overnight, and then calcined at 600 °C in air for 3 h to obtain CZLA support. The theoretical mass percentage of Al<sub>2</sub>O<sub>3</sub> in the oxides is 50.0%.

To obtain the Pd/CZLA-Ba mixed oxides prepared by co-precipitation method (co-catBa), the BaO-doped Ce<sub>0.45</sub>Zr<sub>0.45</sub>La<sub>0.1</sub>O<sub>1.95</sub>-Al<sub>2</sub>O<sub>3</sub> (CZLA-Ba) was prepared according to the same process for CZLA; then Pd(NO<sub>3</sub>)<sub>2</sub> aqueous solution was deposited on CZLA-Ba support materials by incipient wetness method. The obtained sample was dried and calcined at 550 °C for 3 h. The resulting powders were milled with desired deionized water to obtain slurry, then the resulting slurry was washcoated onto a honeycomb cordierite (2.5 cm<sup>3</sup>, the weight was 1.1 g, Corning, America). The loading of washcoat was kept about 140 g·L<sup>-1</sup>. The washcoated catalysts were dried at 120 °C for 2 h and calcined at 550 °C for 3 h. Another type of BaO-loaded Pd-Ba/CZLA mixed oxides was obtained by impregnation method (im-catBa). The as-prepared CZLA powders were impregnated in the aqueous solution of Ba(NO<sub>3</sub>)<sub>2</sub> and Pd(NO<sub>3</sub>)<sub>2</sub>. The successive process followed was the same as the process for Pd/CZLA-Ba. The loadings of Pd and BaO relative to support were 2.0wt% and 5.0wt% , respectively. In order to compare, the Pd/CZLA sample without BaO(cat0) was prepared.

### 1.2 Catalysts characterization

Textural properties were evaluated by low t

temperature nitrogen adsorption-desorption on a QUADRASORB SI Automated Surface Area & Pore Size Analyzer (U.S.). The samples were evacuated at 300 °C for 3 h.

X-ray diffraction (XRD) patterns of catalysts were recorded on a DX-1000 X-ray diffractometer operated at 30 kV and 20 mA, using Cu  $K\alpha$  radiation ( $\lambda=0.154$  18 nm). The crystalline phases were identified according to PDF (The Powder Diffraction File) reference data from International Centre for Diffraction Data (ICDD) of Joint Committee on Powder Diffraction Standards (JCPDS).

Hydrogen temperature-programmed reduction ( $H_2$ -TPR) experiments were performed in a self-assembled experimental setup with a thermal conductivity detector. All samples (100 mg) were pretreated in a quartz tubular micro-reactor in a flow of pure  $N_2$  at 500 °C for 1 h, and then cooled down to room temperature. The reduction was carried out in a flow of 5%  $H_2$ -95%  $N_2$  from 200 to 1 000 °C with a heating rate of 8 °C $\cdot$ min $^{-1}$ .

Temperature-programmed desorption of  $NH_3$  ( $NH_3$ -TPD) experiments were carried out in a fixed-bed quartz reactor. A typical sample mass of 80 mg and a gas flow rate of 30 mL $\cdot$ min $^{-1}$  were used during the experiments. The experiment included four stages: (1) degasification of the sample in Ar at 400 °C for 1 h to clear surface, (2) adsorbed 2%  $NH_3$  at room temperature for 1 h, (3) isothermal desorption in Ar at room temperature until no  $NH_3$  was detected and (4) temperature programmed desorption in Ar at 10 °C $\cdot$ min $^{-1}$  up to 550 °C. The detector was a thermal conductivity detector.

The size of the precipitates was observed with transmission electron microscopy (TEM) using a Tecnai G2 F20 S-TWIN apparatus operated at 200 kV.

X-ray photoelectron spectroscopy (XPS) measurements were performed on a spectrometer (XSAM-800, KRATOS Co) using Mg  $K\alpha$  radiation ( $h\nu=1$  486.6 eV) under ultra-high vacuum condition. The binding energy was determined by reference to the C1s binding energy of 284.8 eV.

### 1.3 Activity evaluation

The catalytic purification for methanol exhaust

was evaluated in a continuous flow fixed-bed reactor by passing mixed gases similar to the gasohol exhaust, and the gases were regulated using mass-flow controllers. The simulated exhaust gas was a mixture of 0.5%~0.6% CO, 0.07%~0.08 %  $C_3H_8$ , 0.08%~0.09% NO, 1.9%~2.2%  $O_2$ , 0.02%~0.03% methanol, and  $N_2$  as the balance gas. The gas space velocity was 30 000 h $^{-1}$ . The organic reaction products were analyzed by gas chromatography (GC-2000, China) equipped with FID detector and a Porapak-Q column. The concentrations of CO, HC, NO,  $O_2$  and  $CO_2$  were analyzed online by a five-component FGA-4001.

## 2 Results and discussion

### 2.1 XRD

The XRD patterns of Ba-modified Pd/CZLA are shown in Fig.1.

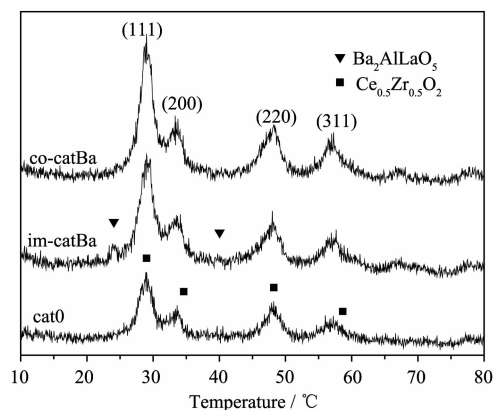


Fig.1 XRD patterns of Pd/CeO $_2$ -ZrO $_2$ -La $_2$ O $_3$ -Al $_2$ O $_3$  (Pd/CZLA) doped by BaO

As seen from Fig.1, all of the diffractograms show the main reflections typical of a cubic fluorite-structured material, with  $fcc$  unit cells at 29.0°, 33.6°, 48.2°, and 58.6°, corresponding to the (111), (200), (220) and (311) planes [14,19]. For co-catBa, no diffraction peaks for BaO are detected, indicating that Ba $^{2+}$  ions are doped into CeO $_2$ ZrO $_2$  framework forming homogeneous CeO $_2$ -ZrO $_2$  solid solutions. Based on Braggs law and Scherrer formula, the lattice parameters and crystallite sizes of all samples are calculated and the results are listed in Table 1. It can be observed that the lattice parameter of co-catBa is larger than that of cat0. The ionic radius of Ba $^{2+}$

**Table 1 Textural and structural properties of Pd/CZLA mixed oxides doped by BaO**

Samples	$S_{\text{BET}} / (\text{m}^2 \cdot \text{g}^{-1})$	$V_s / (\text{mL} \cdot \text{g}^{-1})$	Rmean / nm	Lattice parameter / nm	Mean crystal size / nm
cat0	276	0.28	5.1	0.532 6	4.3
im-catBa	192	0.33	7.9	0.523 8	4.1
co-catBa	147	0.22	7.4	0.534 5	4.6

Lattice parameter is derived from (111), (200), (220) and (311) planes based on Bragg's law

Crystal size is derived from (111) peaks based on Scherrer Equation

(0.134 nm) is larger than that of  $\text{Ce}^{4+}/\text{Ce}^{3+}$  (0.097 nm/0.114 nm) or  $\text{Zr}^{4+}$  (0.084 nm). Therefore, the addition of  $\text{Ba}^{2+}$  into the  $\text{CeO}_2\text{-ZrO}_2$  lattice will result in lattice expansion. However, the lattice parameter of im-catBa is smaller than that of cat0. The diffraction peak reveals the phase segregation for the mixed oxide, with the presence of characteristic  $\text{Ba}_2\text{AlLaO}_5$  phase peaks. It may be resulted from the fact that due to bigger radius of  $\text{La}^{3+}$  (0.106 nm) than that of  $\text{Ce}^{4+}$ , a portion of  $\text{La}^{3+}$  ions has been extracted from the mixed oxides and combined with  $\text{Ba}^{2+}$  forming the  $\text{Ba}_2\text{AlLaO}_5$ , which leads to the significant lattice shrinkage of im-catBa. The similar result has been reported by other groups<sup>[20]</sup>. The XPS results in the following discussion will give more details on this point. So, it can be considered that co-precipitation method will lead to most  $\text{Ba}^{2+}$  ions into the  $\text{CeO}_2\text{-ZrO}_2$  lattice, while the impregnation method can lead to the most  $\text{Ba}^{2+}$  ions remaining on the surface of samples. Besides, no visible PdO or metallic Pd is present in the XRD patterns for all the catalysts, indicating that the content of Pd is too low to be detected or that the Pd particles are well dispersed on the supports.

## 2.2 Nitrogen adsorption-desorption

The textural properties of Pd catalysts modified by BaO with different methods are summarized in Table 1. As shown in Table 1, BET specific surface area of the im-catBa and co-catBa catalyst is  $192 \text{ m}^2 \cdot \text{g}^{-1}$  and  $147 \text{ m}^2 \cdot \text{g}^{-1}$ , smaller than that of cat0 ( $276 \text{ m}^2 \cdot \text{g}^{-1}$ ). But the average pore diameters are obviously affected and even increased from 5.1 nm to 7.9 nm (im-catBa) and 7.4 nm (co-catBa), respectively. This reveals that the introduction of BaO by two methods does not increase the surface area of samples but can broaden the average pore diameter. The cumulative

pore volume of im-catBa is  $0.33 \text{ mL} \cdot \text{g}^{-1}$ , higher than that of co-catBa ( $0.22 \text{ mL} \cdot \text{g}^{-1}$ ). This phenomenon may be resulted from the blocking of small pores or the formation of larger ones. It is confirmed by the increase of the average pore diameter. The same conclusion is also reported in ref. <sup>[21]</sup>. Moreover, previous studies consider that this result can be explained by the formation of new phases<sup>[22]</sup>. So the increased pore volume may be resulted from the presence of  $\text{Ba}_2\text{AlLaO}_5$  as detected by XRD. The bigger pore volume and average pore diameter are beneficial to the adsorption/desorption of reaction species, leading to an improvement of the catalytic activity. This is further confirmed by the result of the catalytic performance of the material. In summary, the textural properties of Pd catalyst are enhanced by two different preparation methods and the impregnation method is superior to co-precipitation method.

## 2.3 $\text{H}_2$ -TPR

The TPR profiles of catalysts are shown in Fig.2. The TPR profile of cat0 shows two peaks  $\beta$  and  $\gamma$  at 150 °C and 300 °C, which are associated with the reduction of PdO species and surface oxygen of  $\text{CeO}_2$ <sup>[23]</sup>. In the case of BaO modified catalysts, the intensity of the peaks over low-temperature is increased with a simultaneous decrease of the intensity of the peak  $\gamma$ . And the reduction temperatures of peaks also shift to lower temperatures. There is a direct correlation between the peak area and the amount of reductive species. The reduction peak areas of co-catBa and im-catBa are larger than that of cat0. These demonstrate that the addition of  $\text{Ba}^{2+}$  is beneficial for the reduction of PdO species and also can increase the amount of reductive species on the surface of Pd-based catalysts.

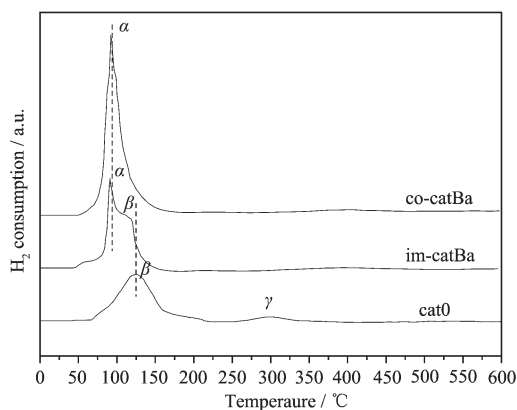


Fig.2  $H_2$ -TPR profiles of Pd/CZLA doped by BaO with impregnation/co-precipitation

Compared with cat0, the im-catBa catalyst shows two peaks  $\alpha$  and  $\beta$  at 80 °C and 110 °C, which is attributed to the reduction of PdO species highly dispersed on the surface of the support and the interaction between PdO and the support [24], respectively. But, unlike the im-catBa catalyst, co-catBa exhibits only one peak  $\alpha$  below 200 °C, and the intensity of  $\alpha$  peak is obviously higher than that of im-catBa. It indicates that the introduction of BaO by co-precipitation clearly promotes the high dispersion of PdO species on the surface of the support and accelerates the reduction rate of PdO. However, the easier reduction of im-catBa and co-catBa has different reasons. For the co-catBa sample, the intensity of reduction peak of PdO specie dispersed on the surface of the support increases obviously. We may attribute this phenomenon to the structural modification in the  $CeO_2$ - $ZrO_2$  lattice when some  $Ce^{4+}$  cations are substituted by  $Ba^{2+}$  leading to the formation of more homogeneous solid solution. This is confirmed by XRD. As reported in refs [25-26], the introduction of  $Ba^{2+}$  in  $CeO_2$ - $ZrO_2$  lattice can induce structure disorder and create additional anion vacancies, thus increasing the oxygen mobility in the bulk of solid solution, causing partial  $O^{2-}$  anion diffusion from bulk to surface, and then increasing the reducibility of Pd catalyst. For the im-catBa sample, two reduction peaks  $\alpha$  and  $\beta$  have been improved, and the shoulder peak  $\beta$  area is distinctly larger than that of peak  $\alpha$ . This fact is mainly associated with the

surface modification. The enrichment of  $Ba^{2+}$  dispersed on the surface of samples prepared by impregnation method will promote the high dispersion of PdO species on the surface of the support, especially strengthen the interaction between PdO and the support. So, except for the highly dispersed PdO, the Pd-Ce interaction species formed in the Pd-Ce interface is another main species. In addition, reference [27] reports that the hydrogen spillover may occur during the PdO reduction and promotes the reduction of  $CeO_2$ -support. The presence of BaO strongly modifies the dispersion of PdO, facilitating diffusion of hydrogen between in PdO particles or PdO particles and the support, which favors the reduction of PdO and the ceria surface.

Based on the above analyses, co-catBa prepared by co-precipitation has a better redox property than im-catBa prepared by impregnation. Different from the co-catBa samples with structural modification, there are two kinds of activity species in the im-catBa sample, such as highly dispersed PdO and the Pd-Ce species formed in the Pd-Ce interface.

#### 2.4 $NH_3$ -TPD

Fig.3 shows the  $NH_3$ -TPD of the samples doped by BaO with different methods. The desorption peak of the cat0 sample not only has the most wide temperature range from 100 °C to 700 °C, but also has the largest peak area. In addition, the  $NH_3$ -TPD profile of un-doped sample exhibits three distinguished desorption peaks  $\alpha$ ,  $\beta$  and  $\gamma$  at 180, 250

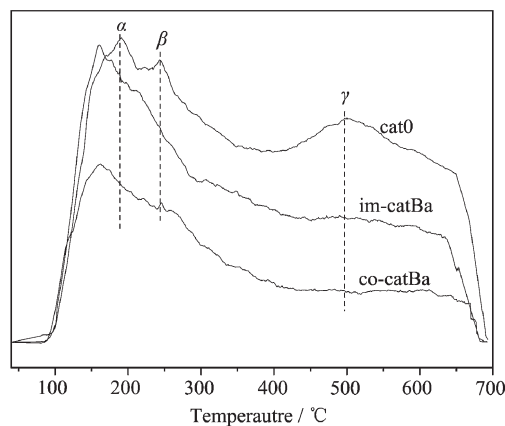


Fig.3  $NH_3$ -TPD profiles of Pd/CZLA doped by BaO with impregnation/co-precipitation

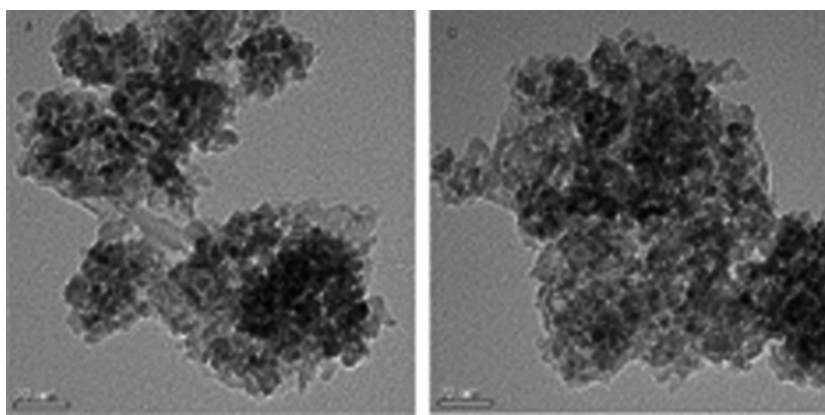
and 500 °C, respectively, which can be ascribed to the  $\text{NH}_3$  desorption of weak acid sites, middle strong acid sites and strong acid sites on the surface of aluminum-containing samples.

As for im-catBa and co-catBa, both the peak temperature and the peak area decrease, and the middle strong acid sites and strong acid sites nearly fade away. This is because that BaO is a basic alkaline compound. The addition of alkaline earth metal oxides will first neutralize some strong and middle strong acid sites on the surface, and then neutralize the weak acid sites, resulting in a decline in the surface acidity. Moreover, the peak area of co-catBa is smaller than that of im-catBa. This may be due to the following reasons: (1) the surface acid sites of catalysts are mainly determined by the number of hydroxyl groups on the surface of aluminum and the aluminum atoms, the more hydroxyl groups and aluminum atoms, the more  $\text{H}^+$  and empty electron orbital<sup>[28]</sup>. Combined with the results of XRD and  $\text{H}_2$ -TPR, it can be inferred that co-precipitation method, leading to almost all of  $\text{Ba}^{2+}$  ions into the CZ lattice, forming homogeneous solid solution, will result maximum neutralization for all acid sites. The impregnation method only modifies the surface of the catalyst by promoting high dispersion of the PdO, which must neutralize part of the surface acid sites; (2)

Furthermore, the amount of surface acidity vary in the order of  $\text{cat0} > \text{im-catBa} > \text{co-catBa}$ . This result corresponds well with the trend of BET specific surface area. According to the principle of  $\text{NH}_3$  adsorption/desorption, the higher surface area for a catalyst, the more surface acid sites. So, the decrease in surface area of im-catBa and co-catBa catalysts is a crucial factor leading to the decline of surface acid sites. The co-catBa has lesser amount of surface acidity than im-catBa.

## 2.5 TEM

TEM images of the catalyst after doping BaO by impregnation/co-precipitation method are shown in Fig. 4. From Fig.4(a) and (b), the average sizes of Pd particle for co-catBa and im-catBa are about 2 and 4 nm, respectively. The dispersion of Pd particles of co-catBa is seemingly higher than that of im-catBa. This may be due to the formation of homogeneous solid solutions as implied by XRD result, which leads to a more compact bond between Pd and the support. So the more highly dispersed Pd particles, the higher reducibility as proved by Wang et al<sup>[24]</sup>. This conclusion is in good agreement with the result of  $\text{H}_2$ -TPR in this work. Therefore, it can be concluded that doping with BaO by co-precipitation is more conducive to the dispersion of Pd particles than by impregnation.



(a) co-catBa; (b) im-catBa

Fig.4 TEM images of Pd/CZLA doped by BaO with impregnation/co-precipitation

## 2.6 XPS

Fig.5(a) and (b) show the XPS spectra of Pd3d and Ce3d after treatment by XPSPEAK, respectively. Table 2 summarizes the binding energy (BE) values

and the surface atomic ratios calculated from XPS.

As shown in Table 2 and Fig.5(a), the binding energies of the Pd3d<sub>5/2</sub> electrons of all catalysts fall in the range of 336.4~337.0 eV. Recent XPS reference

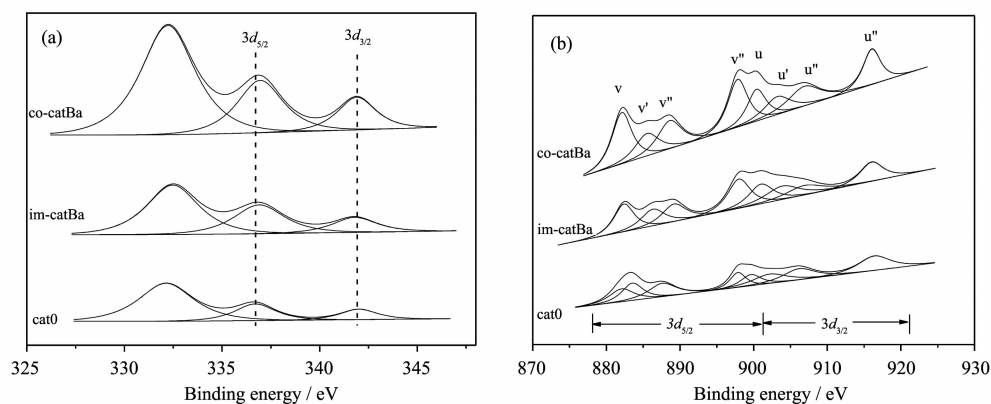


Fig.5 Pd3d (a) and Ce3d (b) XPS spectra of catalysts

Table 2 Binding energy and surface composition results of three catalysts

Catalyst	BE /eV			Surface concentration / at. %					Ce <sup>3+</sup> / (Ce <sup>3+</sup> +Ce <sup>4+</sup> ) / at. %
	Pd3d <sub>5/2</sub>	Ce3d <sub>5/2</sub>	Pd	Al	Ce	La	Zr	Ba	
cat0	336.4	881.8	0.22	23.15	1.29	0.79	1.91	—	22.38
im-catBa	336.9	882.5	0.41	27.36	1.55	1.74	1.94	0.77	25.84
co-catBa	337.0	882.2	0.79	24.08	2.67	1.15	4.64	0.51	26.57

values for the binding energies of PdO and metallic Pd<sup>0</sup> are 336.8 and 335.2 eV, respectively [29]. The binding energy of cat0 Pd3d<sub>5/2</sub> is 336.4 eV, significantly higher than that of Pd<sup>0</sup>, but lower than that of PdO. It indicates that Pd exists in a partly oxidized state. Compared with the cat0, the Pd3d peaks of im-catBa and co-catBa shift to higher BE by 0.5~0.6 eV. As reported in Ref.[30], the addition of BaO could increase the electron density around PdO as an electron donor, resulting in a decrease in the binding energy value, which is in contrast to our results. In this study, the surface atomic ratios of Pd on the cat0, im-catBa and co-catBa are 0.22%, 0.41% and 0.79%, respectively. According to the results of H<sub>2</sub>-TPR and TEM, it can be speculated that the binding energy shift is related with the increase of the Pd species dispersion. Furthermore, the Ce3d<sub>5/2</sub> BE values of im-catBa and co-catBa are all enhanced from 881.8 eV to 882.5 eV and 882.2 eV, respectively. Usually, this phenomenon can be understood as the strong metal-support interaction (SMSI) effect [31]. Unlike co-catBa, the im-catBa sample has more obvious increase for the Ce3d<sub>5/2</sub> BE values by 0.7 eV. This result implies that impregnation

method is more beneficial to promote the Pd-Ce interaction than co-precipitation method. SMSI could change the surface chemical surrounding of PdO and CeO<sub>2</sub> forming chemical bonding such as Pd-O-Ce in the interface of palladium particles and the support. This is consisted with the result of H<sub>2</sub>-TPR.

Fig.5 (b) shows the Ce3d XPS spectra of three samples. The peaks for Ce3d are complex, and they are split into the Ce3d<sub>5/2</sub> and Ce3d<sub>3/2</sub> spin-orbit component of cerium ion. The peaks are assigned as V, V' and V'' for Ce3d<sub>5/2</sub>, while the corresponding Ce3d<sub>3/2</sub> peaks are labeled as U, U' and U'' [32]. According to the literatures [32-33], the peaks at V', U' represent the presence of Ce<sup>3+</sup>, while characteristic peaks of Ce<sup>4+</sup> present at V, V'', V''', U, U'', U'''. As seen from (b), all samples display characteristic peaks of Ce<sup>3+</sup> and Ce<sup>4+</sup>, which indicates that combination of Ce<sup>3+</sup> and Ce<sup>4+</sup> for cerium species coexists in the samples. The concentrations of surface Ce<sup>3+</sup> in the samples, obtained by calculating the relative integrated areas under the curve of each deconvoluted peaks, are shown in Table 2. From Table 2, the concentration of surface Ce<sup>3+</sup> over co-catBa is 26.57%, higher than that of im-catBa (25.84%). The

concentrations of surface  $\text{Ce}^{3+}$  vary in the order of  $\text{co-catBa} > \text{im-catBa} > \text{cat0}$ . The higher the  $\text{Ce}^{3+}$  concentration is, the more  $\text{Ce}^{3+}/\text{Ce}^{4+}$  redox couples are. Therefore, the materials with higher  $\text{Ce}^{3+}$  concentration will possess better redox property. This observation agrees well with the  $\text{H}_2$ -TPR results.

In addition, the quantitative XPS analysis (Table 2) shows a higher concentration of Ce, Zr, especially Al and La ions on the surface of im-catBa than that of cat0 and co-catBa. It further substantiates the formation of  $\text{Ba}_2\text{AlLaO}_5$  compound oxides. Moreover, the higher concentration of Ce and Zr ions on the surface of co-catBa may be related to the substitution  $\text{Ba}^{2+}$  for  $\text{Ce}^{4+}$  and  $\text{Zr}^{4+}$  ions corresponding to the lattice expansion. These results have been confirmed by XRD.

## 2.7 Catalytic performance of catalysts

The catalytic activities of cat0, im-catBa and co-catBa catalysts for conversion of methanol, CO,  $\text{C}_3\text{H}_8$  and NO in the simulated exhaust gas are shown in Fig.6 (a), (b), (c), (d). As seen from Fig.6, the conversion of methanol, CO,  $\text{C}_3\text{H}_8$  and NO over all

catalysts increases continuously with the raising of temperature. Compared (a) and (b), it can be seen that the catalytic activity of co-catBa is lower for methanol conversion, but much higher for CO conversion than that of im-catBa. The data of light-off temperature ( $T_{50}$ ) and complete-conversion temperature ( $T_{90}$ ) obtained from Fig.6 are listed in Table 3. ( $T_{50}$  and  $T_{90}$  are used to evaluate the performances of catalysts. The  $T_{50}$  and  $T_{90}$  are the temperature at which a given pollutant conversion reaches 50% and 90%, respectively.) Compared with cat0, the  $T_{50}$  of CO over co-catBa is  $140^\circ\text{C}$ , while over im-catBa is  $160^\circ\text{C}$ . These phenomena probably relate to the adsorption competition between CO and  $\text{CH}_3\text{OH}$  on the surface of the catalyst. The interaction between the molecular CO and Pd atom can result in strongly adsorbed CO on the surface of Pd catalyst and the formation of the Pd-CO complexes. The strong adsorption of CO on Pd catalyst is unfavorable for methanol oxidation since a dominating adsorption of CO is achieved during the competition adsorption process<sup>[34]</sup>. From  $\text{H}_2$ -TPR, TEM and XPS characterizations, the co-catBa catalyst has

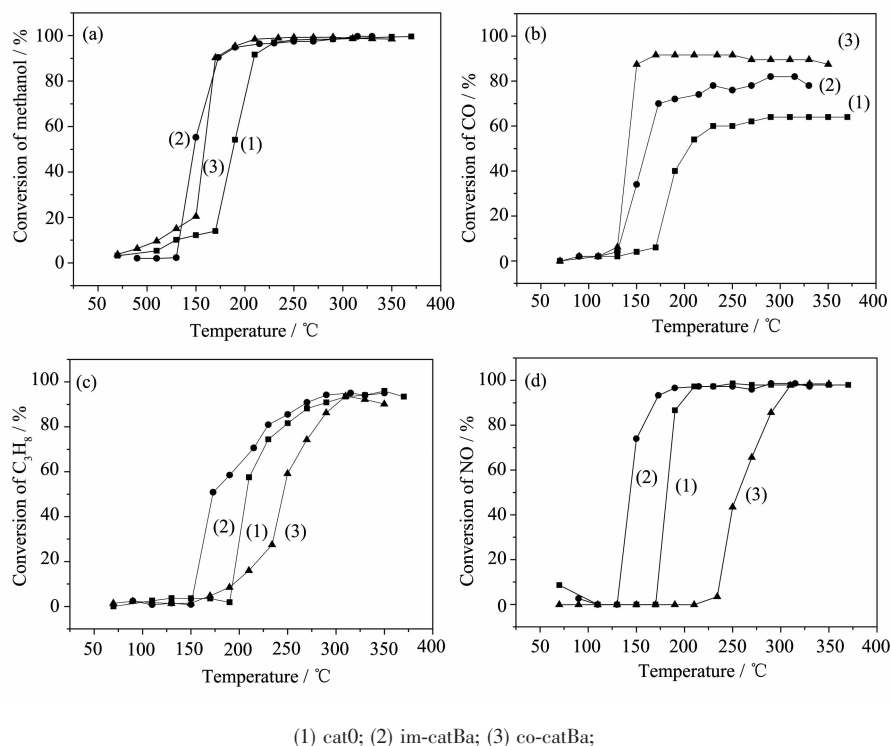


Fig.6 Conversion of methanol (a), CO (b),  $\text{C}_3\text{H}_8$  (c), NO (d) as a function of reaction temperature under stoichiometric  $\text{CH}_3\text{OH}+\text{CO}+\text{C}_3\text{H}_8+\text{NO}+\text{O}_2$

the best reducibility, more highly dispersion, maximum surface  $\text{Ce}^{3+}$  concentration and the most surface atomic ratio of Pd. So, the catalyst co-catBa has the best catalytic activity for CO conversion<sup>[35]</sup>. Differently, the best catalytic activity for  $\text{CH}_3\text{OH}$  conversion over the im-catBa catalyst may be related to the chemical bond Pd-O-Ce formed in the Pd-CZ interface. The doping of CZ into Pd catalyst will generate plenty of oxygen ad-species on the Pd/ $\text{CeO}_2$  interface<sup>[36]</sup>, which can be desorbed and participate in the methanol oxidation at lower temperature. Moreover, Arosio et al.<sup>[37]</sup> demonstrated that the interaction of Pd-Ce bond could contribute to the catalytic activity of Pd/ $\text{CeO}_2$  for the methane oxidation. So it can be inferred that the higher activity for methanol conversion over the im-catBa catalyst is related with the strong Pd-Ce interaction.

Furthermore, we focus on studying  $\text{C}_3\text{H}_8$  and NO, which are the most difficult to convert in exhaust gases from gasoline-methanol vehicles. As seen from Fig.6(c), (d) and Table 3, the trend of catalytic activity for  $\text{C}_3\text{H}_8$  conversion is consistent with NO conversion. The conversion of  $\text{C}_3\text{H}_8$  and NO varies in the order of im-catBa > cat0 > co-catBa. This may be ascribed to the propane-assisted decomposition of NO. Compared with the catalyst cat0, the  $T_{50}$  of  $\text{C}_3\text{H}_8$  and NO over the catalyst im-catBa decreases by 31, 35 °C, but the  $T_{50}$  increases by 35, 75 °C over the catalyst co-catBa. It is obvious that the addition of BaO with the impregnation method can be more effective to improve the catalytic activity, and with the co-precipitation method is negative. The activity for NO reduction is dependent upon the amount of acidity, not just its strength, when saturated hydrocarbons are used as the reducing agent<sup>[38]</sup>. Similarly the surface acidity of catalysts decreases due to the doping of alkaline earth

metals, which causes a decrease in propane conversion<sup>[28]</sup>. So it is speculated that the co-precipitation method resulting the lowest acidity is the important reason leading to the decrease of the  $\text{C}_3\text{H}_8$  and NO conversion.

However, im-catBa has less total acidity, but has better catalytic activity for  $\text{C}_3\text{H}_8$  and NO conversion. This may be resulted from following reasons: 1) it is generally accepted that the NO<sub>x</sub> storage takes place on multiple types of barium sites which have different activities toward NO<sub>x</sub> storage reduction<sup>[39]</sup>. BaO on the Pd-Ba-OSC/ $\text{Al}_2\text{O}_3$  catalyst surface can increase the amount of active sites for NO reactions at low temperature as suggested by Tanja et al.<sup>[40]</sup>. So it can be considered that the formation of  $\text{Ba}_2\text{AlLaO}_5$  phases may be beneficial to the conversion of NO; 2) Pd ions are active sites for NO,  $\text{C}_3\text{H}_8$  adsorption and activation. So the more surface enrichment of Pd species, the higher catalytic activity. On the other hand, the Pd-CZ interface where exists additional sites for oxidant (NO) activation has a direct effect on the NO de-oxidation and  $\text{C}_3\text{H}_8$  oxidation<sup>[41-42]</sup>. From  $\text{H}_2$ -TPR and XPS characterizations, the catalyst im-catBa has more surface enriched Pd species and the Pd-O-Ce species on the Pd-CZ interface due to the surface modification. These may be the crucial factors leading to the excellent catalytic activity towards NO and  $\text{C}_3\text{H}_8$ .

Based on the above analyses, the redox property and highly dispersed PdO species have an important impact on the catalytic performance for CO conversion. The Pd-Ce interaction in the Pd-Ce interface may be the primary factor leading to the excellent catalytic activity towards methanol, NO and  $\text{C}_3\text{H}_8$  conversion.

**Table 3** Light-off ( $T_{50}$ ) and complete-conversion temperature ( $T_{90}$ ) of methanol, CO,  $\text{C}_3\text{H}_8$  and NO over catalysts

Catalyst	$T_{50}$ / °C				$T_{90}$ / °C			
	$\text{CH}_3\text{OH}$	$\text{C}_3\text{H}_8$	CO	NO	$\text{CH}_3\text{OH}$	$\text{C}_3\text{H}_8$	CO	NO
cat0	185	205	205	180	210	285	–	195
im-catBa	142	174	160	145	162	265	–	170
co-catBa	161	240	140	255	170	300	160	300

### 3 Conclusions

The addition of BaO to Pd-based catalyst by impregnation/co-precipitation method greatly improves the textural, redox properties and effectively strengthens the metal-support interaction. The Pd-Ba catalysts exhibit better catalytic performance, and imcatBa is superior to co-catBa. Different synthesis methods modify Pd-based catalyst in different ways. Co-precipitation method is mainly based on the lattice modification when some  $\text{Ce}^{4+}$  cations are substituted by  $\text{Ba}^{2+}$ , causing structure disorder and additional anion vacancies. So, co-precipitation method will cause the formation of more  $\text{Ce}^{3+}$ , accompanied by the creation of more  $\text{Ce}^{3+}/\text{Ce}^{4+}$  redox couples, which leads to a better redox property. The redox property of the catalyst helps the CO conversion. However, impregnation method is mainly based on the surface modification. The enrichment of dispersed  $\text{Ba}^{2+}$  on the surface of the catalyst will promote high dispersion of PdO species on the surface of the support, especially will strengthen the Pd-Ce interaction in Pd-Ce interface of Pd-O-Ce species. The strong Pd-Ce interaction may be beneficial to the conversion of methanol,  $\text{C}_3\text{H}_8$  and NO.

### References:

- [1] Kowalewicz A, Wojtyniak M. *Proc. Inst. Mech. Eng. J. Autom. Eng.*, **2005**,**219**:103-125
- [2] Cenk S, Kadir U, Mustafa C. *Renew. Energy*, **2008**,**33**:1314-1323
- [3] McCabe R W, Mitchell P J. *Appl. Catal.*, **1986**,**27**:83-98
- [4] Mondelli C, Santo D V, Trovarelli A, et al. *Catal. Today*, **2006**,**113**:81-86
- [5] Monte D R, Kaspar J, Fornasiero P, et al. *Inorg. Chim. Acta*, **2002**,**334**:318-326
- [6] Kenevey K, Valdivieso F, Soustelle M, et al. *Appl. Catal. B: Environ.*, **2001**,**29**:93-101
- [7] Liotta L F, Longo A, Macaluso A, et al. *Appl. Catal. B: Environ.*, **2004**,**48**:133-149
- [8] Magdalena K, Elbieta T, Bogusaw M, et al. *Appl. Catal. A: General*, **2012**,**445-446**:280-286
- [9] Hungria A B, Browning N D, Erni R P, et al. *J. Catal.*, **2005**,**235**:251-61
- [10] Osorio G P, Moyado S F, Petranovskii V, et al. *Catal. Lett.*, **2006**,**1/2**:110-116
- [11] Vidmar P, Fornasiero P, Kašpar J, et al. *J. Catal.*, **1997**,**171**:160-168
- [12] Tanja K, Ulla L, Katariina R T, et al. *Appl. Catal. A: General*, **2006**,**298**:65-72
- [13] Groppi G, Cristiani C, Lietti L, et al. *Catal. Today*, **1999**,**50**:399-412
- [14] Atribak I, Bueno L A, García G A. *J. Catal.*, **2008**,**259**:123-132
- [15] Martínez A A, Fernández G M, Hungria A B, et al. *Catal. Today*, **2007**,**126**:90-105
- [16] Thammachart M, Meeyoo V, Risksomboon T, et al. *Catal. Today*, **2001**,**68**:53-60
- [17] Damyanova S, Bueno J M C. *Appl. Catal. A: General*, **2003**,**253**:135-141
- [18] Laurent S, Forge D, Port M, et al. *Chem. Rev.*, **2008**,**108**:2064-2067
- [19] Corbos E C, Courtois X, Bion N, et al. *Appl. Catal. B: Environ.*, **2008**,**80**:62-71
- [20] Li G F, Wang Q Y, Zhao B, et al. *J. Mol. Catal. A: Chem.*, **2010**,**326**:69-74
- [21] Corbos E C, Courtois X, Bion N, et al. *Appl. Catal. B: Environ.*, **2007**,**76**:357-367
- [22] Piacentini M, Maciejewski M, Baiker A. *Appl. Catal. B: Environ.*, **2006**,**66**:126-136
- [23] Sun K P, Lu W W, Wang M, et al. *Appl. Catal. A: General*, **2004**,**268**:107-113
- [24] Wang Q Y, Li G F, Zhao B, et al. *J. Hazard. Mater.*, **2011**,**189**:150-157
- [25] Yamazaki S, Matsui T, Ohashi T, et al. *Solid State Ionics*, **2000**,**136-137**:913-919
- [26] Mikulova J, Rossignol S, Gerard F, et al. *J. Solid State Chem.*, **2006**,**179**:2511-2519
- [27] Feio L S F, Hori C E, Damyanova S, et al. *Appl. Catal. A: General*, **2007**,**316**:107-116
- [28] HE Shen-Nan(何胜楠), SHI Zhong-Hua(史忠华), CHEN Yao-Qiang(陈耀强), et al. *Acta Phys.-Chim. Sin.*(物理化学学报), **2011**,**27**(5):1157-1162
- [29] Voogt E H, Mens A J M, Gijzeman O L J, et al. *Surf. Sci.*, **1996**,**350**:21-31
- [30] YAO Yan-Ling(姚艳玲), FANG Rui-Mei(方瑞梅), SHI Zhong-Hua(史忠华), et al. *Chin. J. Catal.*(催化学报), **2011**,**32**:589-594
- [31] Zhao M, Li X, Zhang L H, et al. *Catal. Today*, **2011**,**175**:430-434
- [32] Larachi F, Pierre J, Adnot A, et al. *Appl. Surf. Sci.*, **2002**,

- 195**:236-245
- [33]Hungria A B, Fernández G M, Anderson J A, et al. *J. Catal.*, **2005**,**235**:262-271
- [34]Wang J A, Aguilar R G, Wang R. *Appl. Surf. Sci.*, **1999**, **147**:44-51
- [35]Corbos E C, Courtois X, Bion N, et al. *Appl. Catal. B: Environ.*, **2007**,**76**:357-367
- [36]Luo Y J, Xiao Y H, Cai G H, et al. *Fuel*, **2012**,**93**:533-538
- [37]Arosio F, Colussi S, Trovarelli A, et al. *Appl. Catal. B: Environ.*, **2008**,**80**:335-342
- [38]Armor J N. *Catal. Today*, **1996**,**31**:191-198
- [39]Yang M, Li Y P, Wang J, et al. *J. Catal.*, **2010**,**271**:228-238
- [40]Tanja K, Ulla L, Katariina R T, et al. *Appl. Catal. A: General*, **2006**,**298**:65-72
- [41]Peng N, Zhou J F, Chen S H, et al. *J. Rare Earths*, **2012**,**30**: 342-349
- [42]Fernández G M, Martnez A A, Iglesias J A, et al. *Appl. Catal. B: Environ.*, **2001**,**31**:39-50